Available online at www.sciencedirect.com
SCIENCE DIRECT®
ELSEVIER
Coastal Engineering 51 (2004) 309–321
Coastal Engineering
An International Journal for Coastal, Harbour and Offshore Engineers
www.elsevier.com/locate/coastaleng

Vertical variation in radiation stress and wave-induced current

Huayong Xia[a,b,*], Zongwan Xia[c], Liangsheng Zhu[b,1]

[a] South China Sea Marine Engineering Prospecting Center, State Oceanic Administration, 155 West Xingang Road, Guangzhou 510300, China
[b] South China Sea Institute of Oceanology, Chinese Academy of Sciences, 164 West Xingang Road, Guangzhou 510301, China
[c] South China Sea Branch, State Oceanic Administration, 155 West Xingang Road, Guangzhou 510300, China

Received 22 August 2002; received in revised form 24 February 2004; accepted 26 March 2004
Available online 8 May 2004

Abstract

In this paper, the traditional concept of radiation stress in water waves is extended to its vertical profile in a new technical way. The definition of and calculation formulae for the vertical profile of radiation stress are advanced. The wave-induced currents over a slopping bottom are modeled. In the simulated example, the wave set-up and set-down, and the vertical structure of wave-induced currents inside and outside the surf zone are successfully modeled. The modeled wave set-up and set-down agree well with the analytical results. The model results reveal also two wave-induced vertical circulations with opposite directions; and the flow pattern agrees well with the measurement of a laboratory experiment. The application of radiation stress with vertical variation is expected to play an important role in the studies of near-shore current systems.

Keywords: Vertical variation in radiation stress; 3-D Numerical model; Wave-induced current; Wave set-up and set-down; Surf zone

1. Introduction

Since the advancement of the concept of radiation stress in water waves (it is taken as "radiation stress" for abbreviation hereafter in this paper) by Longuet-Higgins and Stewart (1964), it has played an important role in the studies of near-shore current systems. In theory, this concept has been used in analyses of wave set-up or set-down (Longuet-Higgins and Stewart, 1964), coastal current (Longuet-Higgins, 1970) and rip current (Bowen, 1969). This concept has also been used widely in modeling wave-induced currents (Dippner, 1987; Larson and Kraus, 1991; Badiei and Kamphuis, 1995; Li et al., 1997; Bao and Nishimura, 2000) and wave–current coupling (Ismail, 1984; Cao and Wang, 1993). But the radiation stress defined by Longuet–Higgins and Stewart is a two-dimensional horizontal tensor, hence, the near-shore current must be also regarded as a 2-D plane vector in its calculation when the radiation stress is taken into consideration; i.e., this current velocity is unchanged in vertical direction. In reality, the near-shore current is three-dimensional, and its vertical structure should be considered. Dyhr-Nielsen and Sorensen (1970) found that, in the surf zone, the vertical water circulations exist. The 3-D structure of near-shore current plays an

* Corresponding author. South China Sea Marine Engineering Prospecting Center, State Oceanic Administration, 155 West Xingang Road, Guangzhou 510300, China. Fax: +86-020-84465062.
E-mail addresses: xiahuayong2001@21cn.com (H. Xia), xzw2003@21cn.com (Z. Xia), lszhu@scsio.ac.cn (L. Zhu).
[1] Fax: +86-020-34450543.

0378-3839/$ - see front matter © 2004 Elsevier B.V. All rights reserved.
doi:10.1016/j.coastaleng.2004.03.003

important role in near-shore mud and sand movement, and in the balance of onshore and offshore material transport. Also, the coupling model of wind, wave and current is one of the hot problems of oceanographic study nowadays. If the radiation stress is not taken into account, the overall wave–current coupling is not possible. The traditional 2-D radiation stress cannot be used in 3-D wave–current coupling calculation. In order to calculate 3-D wave-induced current, the vertical structure of radiation stress must be given.

Some scientists tried to solve this problem. For example, Zheng et al. (2000) and Zheng and Yan (2001) cut the vertical wavy water column into three parts: below the wave trough, wave trough to mean water level (MWL, averaged over a wave period) and above MWL. They calculated the vertical profile of residual momentum flux according to the linear wave theory in these three parts respectively. But in their papers, the definition, the deductive steps and its adaptability are all open to question. In fact, the vertical profile of radiation stress, as shown later in this paper, is the sum of wave residual momentum flux and hydrodynamic pressure averaged over a wave period in different depth (see Eq. (6)). In a wave period, however, the average wave surface is just MWL. Therefore, the radiation stress should distribute vertically from bottom only to MWL, but not to the wave level. This is not correctly done in the works of Zheng et al. For example, in the study of wave-induced current, the wave level process should be considered in neither analytical analysis nor numerical simulation; but the radiation stress above MWL defined by Zheng et al. is irrational, and cannot be involved in the wave-induced current models. Supposing that the radiation stress distributes equally in vertical direction, Xie et al. (2001) used the homogeneous values (2-D radiation stress in water waves divided by water depth) to carry out 3-D wave–current coupling calculation. But in reality, the radiation stress is induced by the velocity of water mass and hydrodynamic pressure, and these two components attenuate near exponentially with depth. The radiation stress should not distribute equally in vertical direction. Therefore, that kind of wave–current coupling could not be accurate.

Considering the importance of the vertical structure of radiation stress, in the present paper, the concept of traditional radiation stress is extended to its vertical profile in a new technical way, its definition and calculation formulae are advanced; and they can be used in modeling 3-D wave-induced current.

2. Vertical profile of radiation stress

2.1. Definition

The calculation formulae of traditional radiation stress are deduced from the theory of small-amplitude waves. Similarly, the formulae of its vertical profile are deduced here also from the same theory. Let the x axis locate in MWL, with its positive direction coinciding with the propagating direction of the wave; z axis points upward; D expresses the water depth below MWL (positive value). On the basis of the small-amplitude wave, we have:

$$\eta = a\cos(kx - \omega t), \tag{1}$$

$$u = a\omega \frac{\cosh k(z+D)}{\sinh kD}\cos(kx-\omega t), \tag{2}$$

$$w = a\omega \frac{\sinh k(z+D)}{\sinh kD}\sin(kx-\omega t), \tag{3}$$

$$p = -\rho g z + \rho g a \frac{\cosh k(z+D)}{\cosh kD}\cos(kx-\omega t), \tag{4}$$

where η denotes the wave level; u and w the velocity components in x and z directions, respectively; p the pressure; $k=2\pi/L$ the wave number, where L is the wave length; $\omega=2\pi/T$ the angular frequency, where T is the period; a the wave amplitude; ρ the density of sea water.

The radiation stress defined by Longuet-Higgins and Stewart (1964) is:

$$S_{xx} = \overline{\frac{1}{T}\int_0^T \int_{-D}^{\eta} (\rho u^2 + p)\mathrm{d}z\mathrm{d}t} - \int_{-D}^{0}(-\rho g z)\mathrm{d}z$$
$$= \overline{\int_{-D}^{\eta}(\rho u^2 + p)\mathrm{d}z} - \frac{1}{2}\rho g D^2 \approx E\left(2n - \frac{1}{2}\right), \tag{5}$$

where the overbar is an operator of averaging over a wave period; the wave energy E is:

$$E = \frac{1}{2}\rho g a^2$$

and n is:

$$n = \frac{1}{2}\left(1 - \frac{2kD}{\sinh 2kD}\right).$$

It is worth noting that, the "radiation stress" as defined by Longuet-Higgins and Stewart (1964) is actually not a "stress" (force per unit area) but a depth integration of stress.

Based on Eq. (5), we will define the vertical profile of radiation stress. In the integration term of momentum flux and hydrodynamic pressure of Eq. (5), we make a variable replacement

$$\sigma = \frac{z-\eta}{D+\eta}$$

in the region $[-D, \eta]$, then $\sigma = 0$ at $z = \eta$, and $\sigma = -1$ at $z = -D$. Also, we make a similar replacement $\sigma = z/D$ in the region $[-D, 0]$ for the integration term of hydrostatic pressure without wave impact. Therefore, from Eq. (5), the radiation stress can be expressed as follows:

$$S_{xx} = \frac{1}{T}\int_0^T \int_{-1}^0 (\rho u^2 + p)(\eta + D)\mathrm{d}\sigma\mathrm{d}t + \int_{-1}^0 \rho g \sigma D^2 \mathrm{d}\sigma$$

$$= \frac{1}{T}\int_0^T \int_{-1}^0 (\rho u^2 + p)(\eta/D + 1)\mathrm{d}\sigma D\mathrm{d}t + \int_{-1}^0 \rho g \sigma D \mathrm{d}\sigma D.$$

Exchanging the integration order yields:

$$S_{xx} = \int_{-1}^0 \left[\frac{1}{T}\int_0^T (\rho u^2 + p)(\eta/D + 1)\mathrm{d}t + \rho g \sigma D\right]\mathrm{d}\sigma D.$$

We take the expression between the square brackets as $S_{xx}(\sigma)$:

$$S_{xx}(\sigma) = \frac{1}{T}\int_0^T [\rho u^2 + p](1 + \eta/D)\mathrm{d}t + \rho g \sigma D. \quad (6)$$

Then Eq. (6) can be defined as the vertical profile of radiation stress. The dimension of $S_{xx}(\sigma)$ is really that of stress (force per unit area). The physical meaning is as follows: in waves, the unit-width micro-cell between two sigma water depths of σ_k and σ_{k+1} has an area of $(1 + \eta/D)\Delta\sigma D$ and has a period-averaged area of $\Delta\sigma D$ (shown in Fig. 1); the sum of momentum flux past through it and dynamic pressure force exerted on it is:

$$(\rho u^2 + p)(1 + \eta/D)\Delta\sigma D.$$

Within a wave period, the sum of average momentum flux and dynamic pressure force is:

$$\frac{1}{T}\int_0^T (\rho u^2 + p)(1 + \eta/D)\Delta\sigma D\mathrm{d}t.$$

Divided by the area of the micro-cell under MWL, $\Delta\sigma D$, the average intensity of momentum flux and dynamic pressure at arbitrary sigma depth (relative depth) can thus be given by:

$$\frac{1}{T}\int_0^T (\rho u^2 + p)(1 + \eta/D)\mathrm{d}t.$$

Eq. (6) expresses physically the sum of momentum flux and dynamic pressure averaged in a wave period subtracting the hydrostatic pressure.

Comparison of the expressions of (5) and (6) as well as their physical meanings shows that $S_{xx}(\sigma)$ is a reasonable extension of the tradition radiation stress S_{xx}. Obviously, $S_{xx}(\sigma)$ and S_{xx} have similar physical meanings, but their dimensions are different. The traditional name of S_{xx} is radiation stress even though it is not a stress, and the vertical profile $S_{xx}(\sigma)$ is a "true" radiation stress. Therefore, sometimes in this

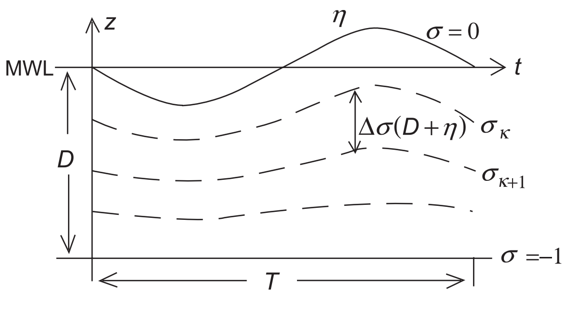

Fig. 1. Integration area in $S_{xx}(\sigma)$ analysis.

paper, we name both of them "radiation stress"; and one can distinguish them from the context without difficulty.

2.2. Calculation formulae of the vertical profile of radiation stress

Let us deduce the calculation formulae of the vertical profile of radiation stress. Spread Eq. (6) and denote:

$$S_{xx}^{(1)}(\sigma) = \overline{\rho u^2},\ S_{xx}^{(2)}(\sigma) = \overline{\rho u^2 \frac{\eta}{D}},$$
$$S_{xx}^{(3)}(\sigma) = \bar{p},\ S_{xx}^{(4)}(\sigma) = \overline{p\frac{\eta}{D}}.$$

Substituting Eq. (2) into $S_{xx}^{(1)}(\sigma)$ yields:

$$S_{xx}^{(1)}(\sigma) = \frac{\rho a^2\omega^2}{\sinh^2(kD)} \times \overline{\frac{\cosh 2k[(1+\sigma)D+(1+\sigma)\eta]+1}{2}\cos^2(kx-\omega t)}$$

$$= \frac{\rho a^2\omega^2}{\sinh^2(kD)}\Big[\cosh 2k(1+\sigma)D \times \overline{\cosh 2k(1+\sigma)\eta\cos^2(kx-\omega t)}/2 + \sinh 2k(1+\sigma)D \times \overline{\sinh 2k(1+\sigma)\eta\cos^2(kx-\omega t)}/2 + 1/4\Big].$$

But

$$\overline{\cosh 2k(1+\sigma)\eta\cos^2(kx-\omega t)} = \sum_{n=0}\frac{1}{(2n)!}[2k(1+\sigma)a]^{2n}\overline{\cos^{2n+2}(kx-\omega t)},$$

$$\overline{\sinh 2k(1+\sigma)\eta\cos^2(kx-\omega t)} = \sum_{n=1}\frac{1}{(2n-1)!}[2k(1+\sigma)a]^{2n-1} \times \overline{\cos^{2n+1}(kx-\omega t)} = 0.$$

In small-amplitude wave, $a \ll L$. Neglect all terms of higher order than ka in the above Taylor expansions (and in the following deductions), then

$$S_{xx}^{(1)}(\sigma) = \frac{\rho a^2\omega^2}{\sinh^2(kD)}[\cosh 2k(1+\sigma)D/4 + 1/4].$$

Substituting the dispersion equation $\omega^2 = gk\tanh kD$ into the above formula yields:

$$S_{xx}^{(1)}(\sigma) = E\frac{k}{\sinh 2kD}[\cosh 2k(1+\sigma)D + 1]. \quad (7)$$

By the same procedure, we can get:

$$S_{xx}^{(2)}(\sigma) = E\frac{3k^2a^2}{2D\sinh 2kD}(1+\sigma)\sinh 2k(1+\sigma)D. \quad (8)$$

In order to deduce $S_{xx}^{(3)}(\sigma)$ and $S_{xx}^{(4)}(\sigma)$, expression for the pressure p must be given. But the pressure given by Eq. (4) is an approximate expression, which is not compatible with Eq. (1). In fact, when Eq. (1) is considered, $p(\eta)=0$ at free surface requires $z=\eta$ in the first term and $z=0$ in the second term on the right-hand side of Eq. (4), which is not rational. Based on the method used by Jiang (1992), we deduce the substitute form of Eq. (4).

Of course, the wave movement satisfies the general fluid dynamics equations. It is a potential motion, and the viscosity can be neglected. In the vertical direction, the momentum equation is:

$$\rho\frac{\partial w}{\partial t} + \rho\frac{\partial uw}{\partial x} + \rho\frac{\partial w^2}{\partial z} = -\frac{\partial p}{\partial z} - \rho g.$$

Integrating this equation in [z, η] and applying the Leibniz equation yield:

$$p(z) = \rho g(\eta - z) - \rho w^2 + \rho\frac{\partial}{\partial t}\int_z^\eta w\mathrm{d}z + \rho\frac{\partial}{\partial x}\int_z^\eta uw\mathrm{d}z - \rho\left[w\left(\frac{\partial\eta}{\partial t} + u\frac{\partial\eta}{\partial x} - w\right)\right]_{z=\eta}.$$

Because at the free surface it satisfies:

$$w(\eta) = \frac{\partial\eta}{\partial t} + u(\eta)\frac{\partial\eta}{\partial x},$$

we have:

$$p(z) = \rho g(\eta - z) - \rho w^2 + \rho\frac{\partial}{\partial t}\int_z^\eta w\mathrm{d}z + \rho\frac{\partial}{\partial x}\int_z^\eta uw\mathrm{d}z. \quad (9)$$

In Eq. (5), the variable replacement for z is just the sigma transformation in coordinate system (Blumberg and Mellor, 1987); and the coordinate transformation from (x, z, t) to (x^*, σ, t^*) is:

$$x^* = x,\ \ \sigma = \frac{z-\eta}{D+\eta},\ \ t^* = t.$$

Suppose in the course of deduction, the sea bottom can be thought of as a horizontal and flat one, by the rule of compound derivation, the derivatives in Cartesian coordinates can be expressed in sigma coordinates as follows:

$$\begin{aligned}\frac{\partial G}{\partial x} &= \frac{\partial G}{\partial x^*} - \frac{\partial G}{\partial \sigma}\left[\frac{\sigma}{D+\eta}\frac{\partial (D+\eta)}{\partial x^*} + \frac{1}{D+\eta}\frac{\partial \eta}{\partial x^*}\right] \\ &= \frac{\partial G}{\partial x^*} - \frac{\partial G}{\partial \sigma}\frac{1+\sigma}{D+\eta}\frac{\partial \eta}{\partial x^*},\end{aligned} \tag{10}$$

$$\begin{aligned}\frac{\partial G}{\partial t} &= \frac{\partial G}{\partial t^*} - \frac{\partial G}{\partial \sigma}\left[\frac{\sigma}{D+\eta}\frac{\partial (D+\eta)}{\partial t^*} + \frac{1}{D+\eta}\frac{\partial \eta}{\partial t^*}\right] \\ &= \frac{\partial G}{\partial t^*} - \frac{\partial G}{\partial \sigma}\frac{1+\sigma}{D+\eta}\frac{\partial \eta}{\partial t^*}.\end{aligned} \tag{11}$$

By the above-mentioned rule of compound derivation, the derivative terms in Eq. (9) can be expressed as follows:

$$\begin{aligned}\rho\frac{\partial}{\partial t}\int_z^\eta w\mathrm{d}z &= \rho\frac{\partial}{\partial t^*}\int_\sigma^0 w(\eta+D)\mathrm{d}\sigma \\ &\quad - \rho\frac{\partial}{\partial \sigma}\int_\sigma^0 w(\eta+D)\mathrm{d}\sigma\frac{\sigma+1}{D+\eta}\frac{\partial \eta}{\partial t^*} \\ &= \rho\frac{\partial}{\partial t^*}\int_\sigma^0 w(\eta+D)\mathrm{d}\sigma + \rho w(\sigma+1) \\ &\quad \times \frac{\partial \eta}{\partial t^*},\end{aligned}$$

$$\begin{aligned}\rho\frac{\partial}{\partial x}\int_z^\eta uw\mathrm{d}z &= \rho\frac{\partial}{\partial x^*}\int_\sigma^0 uw(\eta+D)\mathrm{d}\sigma \\ &\quad - \rho\frac{\partial}{\partial \sigma}\int_\sigma^0 uw(\eta+D)\mathrm{d}\sigma\frac{1+\sigma}{D+\eta}\frac{\partial \eta}{\partial x^*} \\ &= \rho\frac{\partial}{\partial x^*}\int_\sigma^0 uw(\eta+D)\mathrm{d}\sigma \\ &\quad + \rho uw(1+\sigma)\frac{\partial \eta}{\partial x^*}.\end{aligned}$$

Then Eq. (9) can be rewritten as:

$$\begin{aligned}p(\sigma) &= -\rho g\sigma(\eta+D) - \rho w^2 + \rho\frac{\partial}{\partial t^*}\int_\sigma^0 w(\eta+D)\mathrm{d}\sigma \\ &\quad + \rho w(\sigma+1)\frac{\partial \eta}{\partial t^*} + \rho\frac{\partial}{\partial x^*}\int_\sigma^0 uw(\eta+D)\mathrm{d}\sigma \\ &\quad + \rho uw(1+\sigma)\frac{\partial \eta}{\partial x^*}.\end{aligned} \tag{12}$$

For simplicity, the asterisks will be omitted in the following deductions. After a series of complex manipulation each term in $S_{xx}^{(3)}(\sigma)$ becomes:

$$\overline{-\rho g\sigma(\eta+D)} = -\rho g\sigma D,$$

$$\overline{-\rho w^2} = -E\frac{k}{\sinh 2kD}[\cosh 2k(1+\sigma)D - 1],$$

$$\overline{\rho\frac{\partial}{\partial t}\int_\sigma^0 w(\sigma)(\eta+D)\mathrm{d}\sigma} = 0,$$

$$\overline{\rho w(\sigma+1)\frac{\partial \eta}{\partial t}} = E\frac{k(1+\sigma)\sinh k(1+\sigma)D}{\cosh kD},$$

$$\overline{\rho\frac{\partial}{\partial x}\int_\sigma^0 uw(\eta+D)\mathrm{d}\sigma} = \rho\frac{\partial}{\partial x}\int_\sigma^0 (\overline{uw\eta} + \overline{uw}D)\mathrm{d}\sigma = 0,$$

$$\overline{\rho u(\sigma)w(\sigma)(1+\sigma)\frac{\partial \eta}{\partial x}} = -E\frac{k(ka)^2}{2\sinh 2kD}(1+\sigma)^2 \times \cosh 2k(1+\sigma)D.$$

Then $S_{xx}^{(3)}(\sigma)$ can be expressed as:

$$S_{xx}^{(3)} = -\rho g\sigma D - E\frac{k}{\sinh 2kD}[\cosh 2k(1+\sigma)D - 1] + E\frac{k(1+\sigma)\sinh k(1+\sigma)D}{\cosh kD}$$

$$-E\frac{k(ka)^2}{2\sinh 2kD}(1+\sigma)^2\cosh 2k(1+\sigma)D. \quad (13)$$

Similarly, each term in $S_{xx}^{(4)}(\sigma)$ becomes:

$$\overline{-\rho g\sigma(\eta+D)\eta/D} = -\rho g\sigma a^2/(2D) = -E\sigma/D,$$

$$\overline{-\rho w^2\eta/D} = -E\frac{(ka)^2}{2D\sinh 2kD}(1+\sigma)\sinh 2k(1+\sigma)D,$$

$$\overline{\rho\frac{\eta}{D}\frac{\partial}{\partial t}\int_\sigma^0 w(\eta+D)\mathrm{d}\sigma} = \frac{\rho}{D}\overline{\left\{\frac{\partial}{\partial t}[\eta\int_\sigma^0 w(\eta+D)\mathrm{d}\sigma] - \int_\sigma^0\frac{\partial\eta}{\partial t}w(\eta+D)\mathrm{d}\sigma]\right\}} = -\frac{\rho}{D}\int_\sigma^0\overline{\frac{\partial\eta}{\partial t}w(\eta+D)}\mathrm{d}\sigma,$$

$$= -E\frac{(ka^2)}{4D\cosh kD}\int_\sigma^0(1+\sigma)\cosh k(1+\sigma)D\mathrm{d}\sigma - E\frac{k}{\cosh kD}\int_\sigma^0\sinh k(1+\sigma)D\mathrm{d}\sigma,$$

$$= -E\frac{(ka^2)}{4D\cosh kD}\int_\sigma^0(1+\sigma)\cosh k(1+\sigma)D\mathrm{d}\sigma - \frac{E}{D}\left[1 - \frac{\cosh k(1+\sigma)D}{\cosh kD}\right],$$

$$\overline{\rho\frac{\eta}{D}w(\sigma+1)\frac{\partial\eta}{\partial t}} = E\frac{(ka)^2(1+\sigma)^2}{4D\cosh kD}\cosh k(1+\sigma)D,$$

$$\overline{\frac{\rho\eta}{D}\frac{\partial}{\partial x}\int_\sigma^0 uw(\eta+D)\mathrm{d}\sigma} = \frac{\rho}{D}\frac{\partial}{\partial x}\int_\sigma^0\overline{\eta uw(\eta+D)}\mathrm{d}\sigma - \frac{\rho}{D}\int_\sigma^0\overline{\frac{\partial\eta}{\partial x}uw(\eta+D)}\mathrm{d}\sigma$$

$$= \frac{E(ka)^2}{4D\sinh 2kD}\int_\sigma^0\sinh 2k(1+\sigma)D\mathrm{d}\sigma + \frac{Ek^3a^2}{2\sinh 2kD}\int_\sigma^0(1+\sigma)\cosh 2k(1+\sigma)D\mathrm{d}\sigma$$

$$= E\frac{k^2a^2}{4D\sinh 2kD}[\sinh 2kD - (1+\sigma) \times \sinh 2k(1+\sigma)D],$$

$$\overline{\rho uw(1+\sigma)\frac{\eta}{D}\frac{\partial\eta}{\partial x}} = -E\frac{(1+\sigma)(ka)^2}{4D\sinh 2kD}\sinh 2k(1+\sigma)D.$$

Then $S_{xx}^{(4)}(\sigma)$ can be expressed as:

$$S_{xx}^{(4)} = -E\sigma/D - E\frac{(ka)^2}{2D\sinh 2kD}(1+\sigma)\sinh 2k(1+\sigma)D - E\frac{(ka)^2}{4D\cosh kD}\int_\sigma^0(1+\sigma)\cosh k(1+\sigma)D\mathrm{d}\sigma - \frac{E}{D}\left[1 - \frac{\cosh k(1+\sigma)D}{\cosh kD}\right] + E\frac{(ka)^2(1+\sigma)^2\cosh k(1+\sigma)D}{4D\cosh kD} + E\frac{k^2a^2}{4D}\left[1 - \frac{2(1+\sigma)\sinh 2k(1+\sigma)D}{\sinh 2kD}\right]. \quad (14)$$

Combining Eqs. (7), (8), (13) and (14) and the hydrostatic pressure without wave motion, then we have:

$$
\begin{aligned}
S_{xx}(\sigma) = {} & E\frac{k}{\sinh 2kD}[\cosh 2k(1+\sigma)D+1] \\
& + E\frac{3k^2a^2(1+\sigma)}{2D\sinh 2kD}\sinh 2k(1+\sigma)D \\
& - E\frac{k}{\sinh 2kD}[\cosh 2k(1+\sigma)D-1] \\
& + E\frac{k(1+\sigma)\sinh k(1+\sigma)D}{\cosh kD} \\
& - E\frac{k(ka)^2(1+\sigma)^2}{2\sinh 2kD}\cosh 2k(1+\sigma)D - \frac{E\sigma}{D} \\
& - E\frac{(ka)^2(1+\sigma)}{2D\sinh 2kD}\sinh 2k(1+\sigma)D \\
& - E\frac{(ka)^2}{4D\cosh kD}\int_{\sigma}^{0}(1+\sigma)\cosh k(1+\sigma)D\,\mathrm{d}\sigma \\
& - \frac{E}{D}\left[1-\frac{\cosh k(1+\sigma)D}{\cosh kD}\right] \\
& + E\frac{(ka)^2(1+\sigma)^2\cosh k(1+\sigma)D}{4D\cosh kD} + E\frac{k^2a^2}{4D} \\
& \times\left[1-\frac{2(1+\sigma)\sinh 2k(1+\sigma)D}{\sinh 2kD}\right]. \qquad (15a)
\end{aligned}
$$

According to small-amplitude wave theory, those terms higher than ka in Eq. (15a) are small quantities and can be neglected. Hence, Eq. (15a) can be simplified as:

$$
\begin{aligned}
S_{xx}(\sigma) = {} & E\frac{2k}{\sinh 2kD} - \frac{E\sigma}{D} \\
& + E\frac{k(1+\sigma)\sinh k(1+\sigma)D}{\cosh kD} \\
& - \frac{E}{D}\left[1-\frac{\cosh k(1+\sigma)D}{\cosh kD}\right]. \qquad (15b)
\end{aligned}
$$

Integrating $S_{xx}(\sigma)$ in vertical direction yields:

$$
\begin{aligned}
& \int_{-1}^{0} S_{xx}(\sigma)\mathrm{d}\sigma D \\
& = E\frac{2kD}{\sinh 2kD} + \frac{E}{2} + E\left[1-\frac{\sinh kD}{kD\cosh kD}\right] \\
& \quad - E\left[1-\frac{\sinh kD}{kD\cosh kD}\right] = E\left(2n-\frac{1}{2}\right).
\end{aligned}
$$

It can be seen again that $S_{xx}(\sigma)$ defined in Eq. (15b) is the extension of traditional radiation stress.

When there is an angle θ between the x axis and the propagation direction of the wave, the radiation stress can be written as:

$$
\begin{aligned}
S_{xx}(\sigma) = {} & E\frac{k}{\sinh 2kD}[\cosh 2k(1+\sigma)D+1]\cos^2\theta \\
& - E\frac{k}{\sinh 2kD}[\cosh 2k(1+\sigma)D-1] - \frac{E\sigma}{D} \\
& + E\frac{k(1+\sigma)\sinh k(1+\sigma)D}{\cosh kD} \\
& - \frac{E}{D}\left[1-\frac{\cosh k(1+\sigma)D}{\cosh kD}\right], \qquad (16)
\end{aligned}
$$

$$
\begin{aligned}
S_{yy}(\sigma) = {} & E\frac{k}{\sinh 2kD}[\cosh 2k(1+\sigma)D+1]\sin^2\theta \\
& - E\frac{k}{\sinh 2kD}[\cosh 2k(1+\sigma)D-1] - \frac{E\sigma}{D} \\
& + E\frac{k(1+\sigma)\sinh k(1+\sigma)D}{\cosh kD} \\
& - \frac{E}{D}\left[1-\frac{\cosh k(1+\sigma)D}{\cosh kD}\right], \qquad (17)
\end{aligned}
$$

$$
S_{xy}(\sigma) = E\frac{k}{\sinh 2kD}[\cosh 2k(1+\sigma)D+1]\sin\theta\cos\theta, \qquad (18)
$$

$$
S_{yx}(\sigma) = S_{xy}(\sigma). \qquad (19)
$$

And in the Cartesian coordinates, we have:

$$
\begin{aligned}
S_{xx}(z) = {} & E\frac{k}{\sinh 2kD}[\cosh 2k(z+D)+1]\cos^2\theta \\
& - E\frac{k}{\sinh 2kD}[\cosh 2k(z+D)-1] - \frac{Ez}{D^2} \\
& + E\frac{k(z+D)\sinh k(z+D)}{D\cosh kD} \\
& - \frac{E}{D}\left[1-\frac{\cosh k(z+D)}{\cosh kD}\right], \qquad (20)
\end{aligned}
$$

$$S_{yy}(z) = E\frac{k}{\sinh 2kD}[\cosh 2k(z+D)+1]\sin^2\theta - E\frac{k}{\sinh 2kD}[\cosh 2k(z+D)-1] - \frac{Ez}{D^2} + E\frac{k(z+D)\sinh k(z+D)}{D\cosh kD} - \frac{E}{D}\left[1-\frac{\cosh k(z+D)}{\cosh kD}\right], \tag{21}$$

$$S_{xy}(z) = E\frac{k}{\sinh 2kD}[\cosh 2k(z+D)+1]\sin\theta\cos\theta, \tag{22}$$

$$S_{yx}(z) = S_{xy}(z). \tag{23}$$

2.3. Error estimation in shallow waters

In shallow waters, the wavelength becomes short and the product of wave number and amplitude, ka, increases. Eq. (15b) is an equation neglecting terms of higher order than ka in Eq. (15a); the error induced by this neglect is not easy to give analytically. Let us take an example to discuss the errors at breaking point. Suppose the breaker height is 2 m; the breaking depth is determined by the criterion for wave breaking $H=rD$, where $r=0.83$ may be taken as the breaker height index; the wavelength is derived by the dispersion relationship of small-amplitude wave theory. Define such a relative error in percentage |(Eq. (15a) – Eq. (15b))/Eq. (15b)| × 100. These errors, associated with the wave periods of 5, 6 and 7 s, are shown in Fig. 2. It can be seen that, in the scope of theory of small-amplitude wave, the errors of Eq. (15b) are within an allowable range.

In deep waters, the small-amplitude wave can describe the waves well. But in shallow waters, especially in the surf zone, the finite-amplitude wave and Cnoidal wave describe the waves better. Those two kinds of wave theory ought to be used to estimate the error for the present form (Eq. (15b)) and even to deduce the expression of radiation stress in shallow waters. However, these two kinds of waves have much more complicated mathematic forms than the small-amplitude wave. It is difficult to derive the expressions of radiation stress based on the two kinds of wave theory, and even to give explicit expressions based on

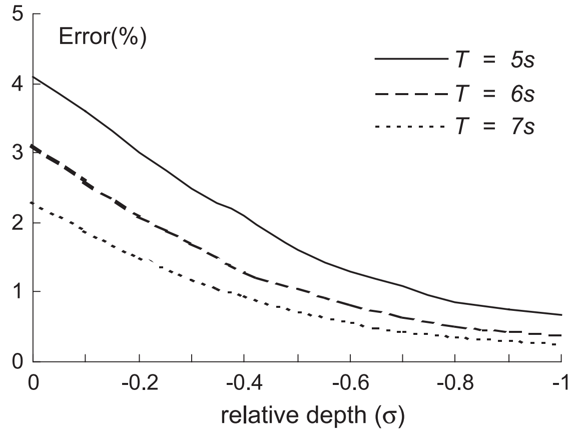

Fig. 2. Error estimation in Eq. (15b), based on the linear wave theory.

the Cnoidal wave theory. The relevant researchers will remain to the future.

In the previous application works on the traditional radiation stress, some verifications show that the theoretical and numerical calculations of wave set-up or set-down and nearshore currents induced by traditional radiation stress agree with the observations (Bowen et al., 1968; Larson and Kraus, 1991; Badiei and Kamphuis, 1995). The analysis of its vertical profile is just an extension of the traditional concept, and the present expression of radiation stress might be an acceptable approximation even in shallow waters.

2.4. Vertical variation in radiation stress

Differentiate radiation stress $S_{xx}(\sigma)$ in vertical direction, we have:

$$\frac{\partial S_{xx}(\sigma)}{\partial\sigma} = \frac{E}{D}\left[-1+\frac{2kD\sinh k(1+\sigma)D}{\cosh kD} + \frac{k^2D^2(1+\sigma)\cosh k(1+\sigma)D}{\cosh kD}\right].$$

In the area $[-1, 0]$, the derivative of $S_{xx}(\sigma)$ is an increasing function. And

$$\frac{\partial S_{xx}(-1)}{\partial\sigma} = -\frac{E}{D},\ \ \sigma=-1;$$

$$\frac{\partial S_{xx}(0)}{\partial\sigma} = \frac{E}{D}\left[-1+2kD\tanh(kD)+(kD)^2\right],\ \ \sigma=0.$$

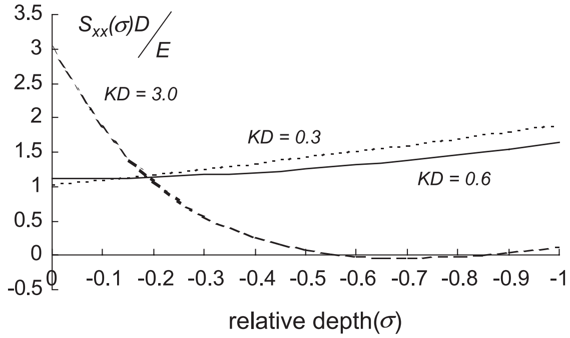

Fig. 3. Radiation stress varying with depth.

Let us examine the equation $x^2+2x\tanh x-1=0$, whose left-hand side is just the expression between the square brackets of the above formulae with $kD=x$. It has a root of 0.6. Namely, when $kD=0.6$, $\partial S_{xx}(0)/\partial\sigma=0$. Therefore, when $kD\leq 0.6$, $S_{xx}(\sigma)$ decreases from the bottom to surface, with the maximum in bottom and minimum in surface. When $kD>0.6$, $S_{xx}(\sigma)$ has a minimum; from this extreme-value point, $S_{xx}(\sigma)$ increases both to the surface and bottom. Fig. 3 shows the vertical variation in $S_{xx}(\sigma)$. It shows that when kD is large the radiation stress reaches its maximum at the surface and decreases rapidly with depth. It agrees with the attenuation rule of the deep-water wave elements of velocity and dynamic pressure. It also shows that the radiation stress has very small, even minus value (with opposite direction to the wave propagation) below half depth.

3. Vertical variation of wave-induced currents

3.1. System of governing equations

In order to model 3-D wave-induced current the hydrodynamic equations used by Xie et al. (2001) are adopted, which are based on the equations of fluid dynamics in sigma coordinates (Blumberg and Mellor, 1987); but the baroclinic pressure terms in the momentum equations are neglected and the radiation stress terms are replaced by the present forms. The governing equations are as follows:

$$\frac{\partial\zeta}{\partial t}+\frac{\partial uD}{\partial x}+\frac{\partial vD}{\partial y}+\frac{\partial w'}{\partial\sigma}=0, \tag{24}$$

$$\begin{aligned}&\frac{\partial uD}{\partial t}+\frac{\partial u^2D}{\partial x}+\frac{\partial uvD}{\partial y}+\frac{\partial uw'}{\partial\sigma}+gD\frac{\partial\zeta}{\partial x}\\&=\frac{\partial}{\partial\sigma}\left[\frac{K_{\mathrm{M}}}{D}\frac{\partial u}{\partial\sigma}\right]+\frac{\partial}{\partial x}\left[2A_{\mathrm{M}}D\frac{\partial u}{\partial x}\right]\\&+\frac{\partial}{\partial y}\left[A_{\mathrm{M}}D\left(\frac{\partial u}{\partial y}+\frac{\partial v}{\partial x}\right)\right]-\frac{1}{\rho}\frac{\partial DS_{xx}(\sigma)}{\partial x}\\&-\frac{1}{\rho}\frac{\partial DS_{xy}(\sigma)}{\partial y},\end{aligned} \tag{25}$$

$$\begin{aligned}&\frac{\partial vD}{\partial t}+\frac{\partial uvD}{\partial x}+\frac{\partial v^2D}{\partial y}+\frac{\partial vw'}{\partial\sigma}+gD\frac{\partial\zeta}{\partial y}\\&=\frac{\partial}{\partial\sigma}\left[\frac{K_{\mathrm{M}}}{D}\frac{\partial v}{\partial\sigma}\right]+\frac{\partial}{\partial y}\left[2A_{\mathrm{M}}D\frac{\partial v}{\partial y}\right]\\&+\frac{\partial}{\partial x}\left[A_{\mathrm{M}}D\left(\frac{\partial u}{\partial y}+\frac{\partial v}{\partial x}\right)\right]-\frac{1}{\rho}\frac{\partial DS_{yy}(\sigma)}{\partial y}\\&-\frac{1}{\rho}\frac{\partial DS_{yx}(\sigma)}{\partial x},\end{aligned} \tag{26}$$

where $\zeta(x, y, t)$ is the sea surface elevation, which is equal to MWL; u and v the current speed in x and y directions, respectively; A_{M} and K_{M} the horizontal and vertical eddy viscosity, respectively; w' the vertical speed in sigma coordinates.

The boundary conditions for momentum equations are as follows: At the free surface

$$\rho_0\frac{K_{\mathrm{M}}}{D}\left[\frac{\partial u}{\partial\sigma},\frac{\partial v}{\partial\sigma}\right]=(\tau_{\mathrm{a}x},\tau_{\mathrm{a}y}),\quad \sigma\to 0,$$

where τ_{a} is the surface wind stress. It is taken as zero in calculation of wave-induced current. At the bottom, when the wave effect is not taken into account, the boundary condition is:

$$\frac{K_{\mathrm{M}}}{D}\left[\frac{\partial u}{\partial\sigma},\frac{\partial v}{\partial\sigma}\right]=c_z(u^2+v^2)^{1/2}(u,v),\quad \sigma\to -1,$$

where

$$c_z=\max\left[k_0^2/\ln^2(z_1/z_0),\ 0.0025\right],$$

$k_0=0.4$ is the von Karman constant; z_0 the bottom roughness; z_1 the distance between the bottom and the center of the lowest grid. In the calculation of wave-induced current the friction caused by waves should be added, and the formulae for wave–current friction coefficient are very complicated (Lou and Ridd, 1996). In the following simulation case, the waves play a predominant role in the bottom stress. For simplicity, only the wave friction factor is used (Swart, 1974):

$$f_w = \exp\left[5.213\left(\frac{k_s}{A_b}\right)^{0.194} - 5.977\right],\ f_{w\max} = 0.3,$$

where k_s is the effective bottom roughness height; A_b the near-bottom excursion amplitude. Thus, c_z is taken as $f_w/2$. We calculate the bottom friction in the light of treating the bottom stress for 2-D wave-induced current. Denote the two horizontal velocity components of wave as u_w and v_w, then the instantaneous speed of water can be expressed as $U = u + u_w$, $V = v + v_w$. Then we have:

$$[\tau_{bx}, \tau_{by}] = -\rho c_z (U^2 + V^2)^{1/2}(U, V), \quad \sigma \to -1,$$

$$[\bar{\tau}_{bx}, \bar{\tau}_{by}] = -\rho c_z \frac{1}{T}\int_0^T (U^2 + V^2)^{1/2}(U, V)\mathrm{d}t, \quad \sigma \to -1.$$

Because the distance between the center of the lowest grid and the bottom is small, in these two formulae, the horizontal speed of the water mass in a wave at this mesh center is substituted by the water speed at bottom. For simplicity, the bottom friction is calculated by using the absolute average speed of the water mass in a wave at the bottom:

$$u_w(-1) = \frac{a\omega}{\sinh kD}\cos(kx - \omega t)\cos\theta,$$
$$v_w(-1) = \frac{a\omega}{\sinh kD}\cos(kx - \omega t)\sin\theta,$$

$$\overline{|u_w(-1)|} = \frac{2}{\pi}\frac{a\omega}{\sinh kD}\cos\theta,$$
$$\overline{|v_w(-1)|} = \frac{2}{\pi}\frac{a\omega}{\sinh kD}\sin\theta.$$

Denoting:

$$\alpha = (u + \overline{|u_w|})^2 + (v + \overline{|v_w|})^2,$$
$$\beta = (u - \overline{|u_w|})^2 + (v - \overline{|v_w|})^2,$$

we then have:

$$\bar{\tau}_{bx} = -\rho c_z \frac{1}{T}\left[\int_0^{\frac{T}{2}} (u + \overline{|u_w|})\sqrt{\alpha}\mathrm{d}t + \int_{\frac{T}{2}}^{T} (u - \overline{|u_w|})\sqrt{\beta}\mathrm{d}t\right] = -\frac{\rho c_z}{2}[u(\sqrt{\alpha} + \sqrt{\beta}) + \overline{|u_w|}(\sqrt{\alpha} - \sqrt{\beta})], \tag{27}$$

$$\bar{\tau}_{by} = -\rho c_z \frac{1}{T}\left[\int_0^{\frac{T}{2}} (v + \overline{|v_w|})\sqrt{\alpha}\mathrm{d}t + \int_{\frac{T}{2}}^{T} (v - \overline{|v_w|})\sqrt{\beta}\mathrm{d}t\right] = -\frac{\rho c_z}{2}[v(\sqrt{\alpha} + \sqrt{\beta}) + \overline{|v_w|}(\sqrt{\alpha} - \sqrt{\beta})], \tag{28}$$

As for the horizontal eddy viscosity, the method used by Longuet-Higgins (1970) is adopted; i.e., $A_M = N|x|\sqrt{gD}$, where N is a non-dimensional coefficient, with a value of 0–0.016; x the distance to the coastline.

As for the vertical eddy viscosity, take:

$$K_M = v + v_w, \tag{29}$$

where v is the common vertical viscosity and v_w is the viscosity caused by wave. The calculation of v follows Zhu and Fang (1994):

$$v = v_0 + l^2\left[\left(\frac{\partial u}{\partial z}\right)^2 + \left(\frac{\partial v}{\partial z}\right)^2\right]^{\frac{1}{2}}, \tag{30}$$

where v_0 is the molecular viscosity; l the mixing length:

$$l = k_0(z' - z_0)\left[1 - \frac{z'}{(1+s)D}\right],$$

where $s = 0.1$ the parameter denoting the surface roughness; $z' = z + D$ the distance to the bottom.

The calculation of v_w follows Башкиров (after Wang, 1984):

$$v_w = \frac{bgTH\cosh k(z+D)}{4\pi\cosh kD}, \tag{31}$$

where H is the wave height; $b = 0.0025$ a parameter from experiment.

The splitting technique used by Xia et al. (1997) is adopted for the model's calculation. Because the Coriolis force is not considered in the wave-induced current, the predictor–corrector scheme for Coriolis force term used in the above-mentioned reference is omitted here.

3.2. An example of wave-induced current calculation

In this paper, only one example of wave-induced current modeling is given. In this example, simple bottom topography and normally incident waves are considered, and the currents are just vertically two-dimensional. The foregoing 3-D model is of course competent for this modeling. The reason why we choose this example is that there exist an analytical solution describing the wave set-up or set-down and a laboratory measuring result describing vertical currents profiles in the similar case, which can be used to examine the present model.

Longuet-Higgins and Stewart (1964) gave an analytical solution of wave set-up or set-down on a straight and gently sloping beach, with the waves coming into the shore normally. In that paper, assumptions are as follows:

$$\frac{dS_{xx}}{dx} = -\rho gD\frac{d\zeta}{dx}; \tag{32}$$

outside the surf zone $dEC_g/dx = 0$, where C_g is group speed; inside the surf zone the wave height $H = rD$, where $r = 0.83$. Under these assumptions, the wave sets down outside the surf zone and sets up inside the surf zone with the function:

$$\zeta = -\frac{H^2K}{8\sinh 2kD} \tag{33}$$

and

$$\zeta = \left(1 + \frac{8}{3r^2}\right)^{-1}(D_B - D) + \zeta_B, \tag{34}$$

respectively, where D_B and ζ_B are respectively the water depth and the value of wave set-down at the breaking point.

Bijker et al. (1974) measured the mass transport in a laboratory experiment. They also measured vertical current profile on a sloping beach. We will simulate one of their experiments by using the model described in this sub-section. The modeled wave set-up and set-down will be compared with the analytical solutions of Eqs. (33) and (34), while the modeled vertical current profiles will be compared with Bijker's observations.

The wave condition follows case "Wave 5" in Bijker's experiments. In that run, the beach slope was 1:10; the water depth out of the sloping part was constant with 0.45 m; the height of incident deep-water wave 0.181 m; the wave period 1.5 s. At the bottom, there are artificial symmetrical ripples with the length of 80 mm and the height of 18 mm. In the model, the x axis is perpendicular to the shore, with the origin at the coastline. The model area is 9 m in x direction; the horizontal grid 0.125 m; the vertical space step $\Delta\sigma = 0.125$; the calculation period 1 h; the time step 0.002s. The effective bottom roughness height k_s is calculated as follows (van Rijn, 1984):

$$k_s = 1.1H_r\left[1 - \exp\left(-25\frac{H_r}{L_r}\right)\right],$$

where H_r is the ripple height and L_r the ripple length. The modeled results are shown in Figs. 4 and 5.

It can be seen in Fig. 4 that the modeled result coincides reasonably well with the analytical solution. The modeling also shows that outside the breaking point the waves cause MWL to fall with the maximum set-down at this point; inside the surf zone the waves cause MWL to increase linearly from the lowest point.

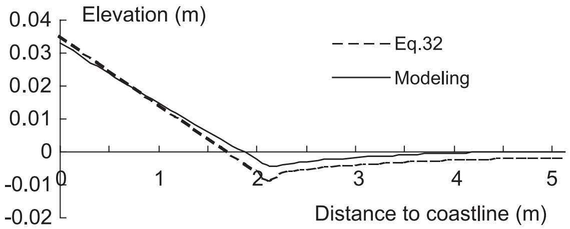

Fig. 4. Wave-induced set-up or set-down.

The modeled maximum wave set-up and set-down is a bit smaller than the corresponding analytical solution respectively, perhaps due to the omission of the bottom friction in Eq. (32). If bottom shear stress is induced in Eq. (32),

$$\frac{\mathrm{d}S_{xx}}{\mathrm{d}x} = -\rho g D \frac{\mathrm{d}\zeta}{\mathrm{d}x} - \tau_{\mathrm{B}}, \tag{35}$$

the agreement may be better. In fact, it can be seen in Fig. 5 that, inside the surf zone, the wave-induced bottom current is onshore; and the bottom friction direction is in the opposite direction. If the bottom friction is omitted, there will be a larger barotropic gradient to balance the radiation stress gradient.

The vertical sections of modeled current are shown in Fig. 5. The wave-induced current forms two vertical circulations with opposite directions, which are bounded on the breaking point. Outside the surf zone, the surface water flows onshore, the bottom water flows offshore, and strong downwelling happens near the breaking point. Inside the surf zone, the current speed is smaller than outside, and the flow pattern is just opposite: The surface water flows offshore, the bottom water flows onshore and strong downwelling happens also near the breaking point. These movements are compatible with the surface slope.

The modeled flow pattern agrees well with Bijker's measurement of laboratory experiment, and the vertical profiles are similar. Outside the surf zone, the modeled currents have the same order of magnitude as the measurement. And both model and observation show that the water flows onshore in a thinner upper layer and flows offshore in a thicker bottom layer.

The patterns of wave-induced current in the surf zone are complex. For example, the reverse flow pattern in vertical section, so-called undertow in surf zone was reported (Svendsen et al., 1987) and Deigaard et al. (1991) pointed out that, other than the radiation stress, there are different factors that can influence the vertical flow patterns. These different vertical current patterns in surf zone show that further studies are needed.

4. Conclusion

In this paper, the concept of the radiation stress in water waves is extended to its vertical profile. A clear definition of and the calculation formulae for the vertical profile of radiation stress are advanced, which can be well used in 3-D wave–current coupling. In a case for the sloping beach and normally incident waves, the vertical 2-D wave-induced currents are simulated. In this calculated example in vertical section inside and outside the surf zone, the modeled

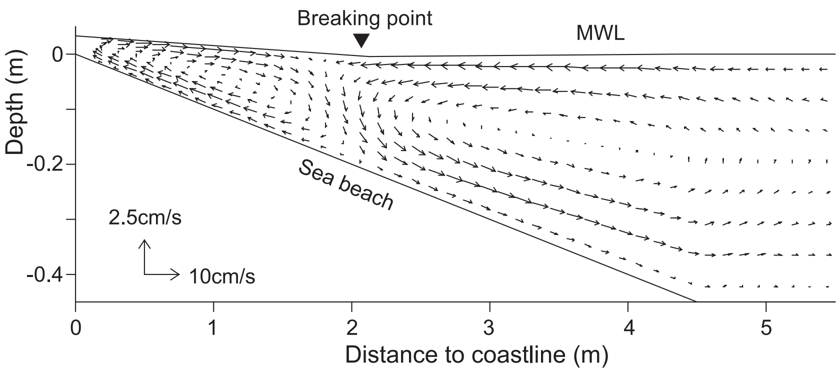

Fig. 5. Wave-induced current inside and outside the surf zone.

water level agrees well with the analytical result, and the modeled currents show two vertical circulations, which agree well with that measured in a laboratory experiment.

In this paper, only a calculated example of wave-induced currents over a sloping bottom is given. For many other topics, such as coastal current, rip current, wave-induced current over complex topography, as well as material transport in near-shore waters, etc., we hope to carry out more model studies in the future.

Acknowledgements

This work is jointly sponsored by the Nature Science Funds of State Oceanic Administration of China in 2001 and by the Science and Technology Funds of Chinese Academy of Sciences under contract No. CXJJ-28. The authors wish to thank the support of these funds.

References

Badiei, P., Kamphuis, J.W., 1995. Physical and numerical study of nearshore currents. Proc. Coastal Dynamics'95. ASCE, Gdańsk, Poland, pp. 377–388.

Bao, S., Nishimura, H., 2000. A new model for analyses of near-shore current. Acta Oceanologica Sinica 22 (5), 115–123 (in Chinese).

Bijker, E.W., Kalwijk, J.P.Th., Pieters, T., 1974. Mass transport in gravity waves on a sloping bottom. Proc. 14th Conf. Coastal Engineering, vol. 2. ASCE, New York, pp. 447–465.

Blumberg, A., Mellor, G., 1987. A description of a three dimensional ocean circulation. In: Heaps, N.S. (Ed.), Three Dimensional Coastal Ocean Model. AGU, Washington, DC, pp. 1–16.

Bowen, A.J., 1969. Rip currents: 1. Theoretical investigations. Journal of Geophysical Research 74 (23), 5467–5478.

Bowen, A.J., Inman, D.L., Simmons, V.P., 1968. Wave "set-down" and "set-up". Journal of Geophysical Research 73 (8), 2569–2577.

Cao, Z., Wang, G., 1993. A numerical model for sediment entrainment by wave and sediment transport by tidal current. Acta Oceanologica Sinica 15 (2), 107–118 (in Chinese).

Deigaard, R., Justesen, P., FredsØe, J., 1991. Modelling of undertow by a one-equation turbulence model. Coastal Engineering 15, 431–458.

Dippner, J.W., 1987. A swell model of the German Bight. Coastal Engineering 11, 527–538.

Dyhr-Nielsen, M., Sorensen, T., 1970. Some sand transport phenomena on coasts with bars. Proc. 12th Inter. Conf. Coastal Eng., vol. 2. ASCE, New York, pp. 855–865.

Ismail, N.M., 1984. Wave–current models for design of marine structure. Journal of Waterway, Port, Coastal and Ocean Engineering, ASCE 110 (4), 432–447.

Jiang, D., 1992. Dynamics of Ocean Wave. Qingdao Ocean Univ. Press, Qingdao. In Chinese.

Larson, M., Kraus, N.C., 1991. Numerical model of longshore current for bar and trough beaches. Journal of Waterway, Port, Coastal and Ocean Engineering, ASCE 117 (4), 326–347.

Li, R., Meng, X., Wang, L., 1997. The mathematical model to simulate nearshore current of Maidao sewage disposal plant in Qingdao (China). Coastal Engineering 16 (3), 32–40 (Chinese journal).

Longuet-Higgins, M.S., 1970. Longshore currents generated by obliquely incident sea waves, 1. Journal of Geophysical Research 75 (33), 6778–6801.

Longuet-Higgins, M.S., Stewart, R.W., 1964. Radiation stress in water waves: a physical discussion with applications. Deep Sea Research 11, 529–562.

Lou, J., Ridd, P.V., 1996. Wave–current bottom shear stresses and sediment resuspension in Cleveland Bay, Australia. Coastal Engineering 29, 169–186.

Svendsen, I.A., Schäffer, H.A., Hansen, J.B., 1987. The interaction between the undertow and the boundary layer flow on a beach. Journal of Geophysical Research 92 (C11), 11845–11856.

Swart, D.H., 1974. Offshore Sediment Transport and Equilibrium Profiles, vol. 131. Delft Hydraulics Lab., The Netherlands.

van Rijn, L.C., 1984. Sediment transport: part III. Bed forms and alluvial roughness. Journal of Hydraulic Engineering, ASCE 110 (12), 1733–1754.

Wang, S., 1984. Vertical distribution of suspended sediment concentration under wave action. Science in China. Series A, Mathemathics, Physics, Astronomy, & Technological Science 12, 1151–1160 (in Chinese).

Xia, H., Yin, Z., Huo, Z., Chen, M., 1997. 3-D Numerical simulation of tidal currents in the Beibu Gulf. Acta Oceanologica Sinica 19 (2), 21–31 (in Chinese).

Xie, L., Wu, K., Pietrafesa, L., Zhang, C., 2001. A numerical study of wave–current interaction through surface and bottom stresses: wind-driven circulation in the South Atlantic Bight under uniform winds. Journal of Geophysical Research 106 (C8), 16841–16855.

Zheng, J., Yan, Y., 2001. Vertical variations of wave-induced radiation stress tensor. Acta Oceanologica Sinica 20 (4), 597–605.

Zheng, J., Yan, Y., Peng, S., 2000. Vertical distribution of wave-induced excess momentum fluxes. Journal of Hohai University 28 (1), 8–13 (in Chinese).

Zhu, Y., Fang, G., 1994. A 3-D barotropic model of continental shelf and shallow sea circulation and its application to the Bohai Sea, Huanghai Sea and East China Sea. Acta Oceanologica Sinica 16 (4), 12–25 (in Chinese).